ELSEVIER

Toxicon 40 (2002) 917–922

TOXICON

www.elsevier.com/locate/toxicon

Crystal structures of an acidic phospholipase A_2 from the venom of *Naja Kaouthia*

Lichuan Gu[a], Zhiqing Wang[b], Shiying Song[a], Yuyan Shu[b], Zhengjiong Lin[a,*]

[a]*National Laboratory of Biomacromolecules, Institute of Biophysics, Chinese Academy of Sciences, Beijing 100101, People's Republic of China*
[b]*Snake Venom research Institute, Guangxi Medical University, Nanning 530021, People's Republic of China*

Received 16 November 2001; accepted 21 January 2002

Abstract

A phospholipase A_2 purified from the venom of *Naja kaouthia* (Guangxi cobra) exhibits anticoagulant activities. The structures of two crystal forms were determined by X-ray crystallography at 2.8 Å resolution with the *Naja naja* (India cobra) PLA_2 as an initial model. The enzyme exhibits a trimer structure, which is similar to that of India cobra PLA_2. This reinforces the physiological relevance of the oligomer. The trimer has a wide cavity, which allows the substrate to enter and interact with the catalytic site. The formation of the trimer may serve as a storage method to improve the solubility at high concentration in the venom gland. The Ca^{2+} binding loop in the absence of the cation can exist in different conformations depending on its surroundings.

Keywords: *Naja kaouthia* phospholipase A_2; Crystal structure; Multimerisation state; Anticoagulant activitiy

1. Introduction

Phospholipase A_2 (PLA_2s, EC 3.1.1.4) catalyzes the hydrolysis of the fatty acid ester at the sn-2 position of phospholipids with Ca^{2+} as an obligatory cofactor. It is one of the most important enzymes for metabolism of lipids. The low molecular mass secretory PLA_2s are classified into two main groups based on the sequence and structural homology (Heinrikson et al., 1977; Dufton and Hider, 1983). In addition to being a catalyst for the hydrolysis of phospholipids, PLA_2 from snake venom displays various pharmacological activities (Gowda et al., 1994; Betzel et al., 1999) such as neurotoxicity, hemolytic activity, cardiotoxicity, myotoxicity, and anticoagulant and antiplatelet activities.

A number of crystal structures of snake venom PLA_2s from various sources have been determined, including rattlesnake venom (Brunie et al., 1985), Chinese pit viper venom (Wang et al., 1996; Tang et al., 1998), Indian cobra venom (Fremont et al., 1993; Segelke et al., 1998), etc. Some PLA_2s were shown to associate as oligomers in the crystalline state as well as in solution. For example, the rattlesnake venom PLA_2 and the K49 class II myotoxins from *Bothrops asper* (Arni et al., 1995) form dimers, while the Indian cobra venom PLA_2 is trimeric. The molecular mechanism behind this multimerisation and its potential function has been investigated for a long time. It was suggested that some monomeric cobra venom PLA_2 molecules aggregate while complexed with phospholipid (Pluckthun and Dennis, 1985).

Naja kaouthia PLA_2 is a group I enzyme with a molecular weight of about 14 kDa which exhibits anticoagulative activity (Wang, 1999). In this paper we report the crystal structure determination of this PLA_2 in two crystal forms and analyze the oligomer structure and the Ca^{2+} binding loop. The anticoagulant site is also discussed.

2. Materials and methods

2.1. Crystallization and data collection

The PLA_2 enzyme provided for crystallization was extracted from the venom of *N. kaouthia* (collected from Guangxi Province, China) according to the procedure outlined previously (Wang et al., 2001). Crystals were grown at

* Corresponding author. Tel.: +86-202-2029; fax: +86-202-7837.
E-mail address: lin@sun5.ibp.ac.cn (Z. Lin).

0041-0101/02/$ - see front matter
PII: S0041-0101(02)00085-5

Table 1
Refinement results

Space group	$P2_13$	$P4_32_12$
Number of molecules/asym. unit	1	3
Crystallographic *R* factor (%)	20.43	23.07
Crystallographic *R*-free factor (%)	24.89	28.24
Resolution range (Å)	8.0–2.8	8.0–2.8
Number of reflections	2570	10,394
Number of non-H protein atoms	902	2684
Number of solvent molecules	29	89
RMS deviations from ideality		
Bond distances (Å)	0.008	0.008
Bond angles (°)	1.08	1.38
Dihedral angles (°)	25.68	25.42
Improper angles (°)	0.83	0.90

18 °C by the hanging-drop vapor diffusion method with ammonium sulfate or PEG4000 as precipitant and β-OG (octyl-β-D-glycopyranoside) as additive. Two forms of single crystals were found in the drops after 2 weeks. The crystals grown in ammonium sulfate belong to space group $P2_13$ with cell dimensions of $a = b = c = 68.40$ Å and one molecule per asymmetric unit, while the crystals grown in PEG4000 belong to $P4_32_12$ with cell dimensions of $a = b = 87.97$ Å and $c = 108.31$ Å and three molecules per asymmetric unit. The crystal of $P2_13$ contains 55.3% estimated solvent content while the other contains 47.2% estimated solvent content (Matthews, 1968). The detailed crystallization procedure and preliminary X-ray characterization of the crystal were described earlier (Wang et al., 2001).

Data was collected on a Mar 345 research area detector ($\lambda = 1.54178$ Å) using a single crystal at a temperature of 20 °C. The data was scaled and merged using the *HKL* Suite (Otwinowski and Minor, 1997). The data sets have an *R*-merge of 12.2% and completeness of 99% for the $P2_13$ form and *R*-merge of 13.4% and completeness of 99% for the $P4_32_12$ form between 20 and 2.8 Å.

2.2. Structure determination and refinement

N. kaouthia PLA_2 is highly homologous to *Naja naja* PLA_2 with sequence identity of 95% (Joubert and Taljaard, 1980). The two crystal forms of *N. kaouthia* PLA_2 are isomorphous with those of *N. naja* PLA_2 (Fremont et al., 1993; Segelke et al., 1998). Thus the structures were determined by the isomorphous difference Fourier method with the *N. naja* PLA_2 (entry 1A3D and 1A3F in Brookhaven Protein Data Bank) as an initial model.

The refinement was carried out using the CNS program (Brunger et al., 1998) with 10% of the data reserved to calculate the free *R* factor (Brunger, 1992). The cubic structure was refined using 2570 reflections in the resolution range 8.0–2.8 Å. The tetragonal structure was refined against 10,394 reflections from 8 to 2.8 Å. Model rebuilding was carried out with the Turbo/Frodo graphics programs on an O2 workstation. Atomic models were iteratively adjusted according to the $2F_o–F_c$ and $F_o–F_c$ electron density maps. During the course of the refinement, the crystallographic *R* factor was gradually reduced and solvent molecules were gradually included in the model based on their electron densities and environments. After several cycles of atomic position and group *B*-factor refinements and model rebuilding, the *R* values and *R*-free values of the two structures converged with the $F_o–F_c$ map showing no more obvious uninterpretable features.

The final model has good stereochemistry and acceptable RMS deviations from ideal values for bond lengths and bond angles. Calculations by the PROCHECK program (Laskowski et al., 1993) indicated that almost all non-glycine residues in the asymmetric unit were located in the most favored regions or the additional allowed regions. The crystallographic *R* and *R*-free values of both structures are within acceptable ranges. The refinement results are listed in Table 1.

3. Results

3.1. Overall structure

The final model consisted of 902 non-H protein atoms and 29 water molecules for the cubic form, and 2684 non-H protein atoms and 89 water molecules for the tetragonal form. The corresponding $2F_o–F_c$ electron density maps of the two crystal structures were continuous and well defined for both the backbone and the side-chains except for a few polar side-chains on the molecule surface.

As a member of group I PLA_2s, *N. kaouthia* PLA_2 has high homology with *N. naja* PLA_2 (differing by six amino acids) and *Naja atra* PLA_2 (differing by four amino acids). All the differences in the amino acid sequences occur at the molecular surface, leading to similar three-dimensional structures. The *N. kaouthia* PLA_2s monomers have all the structural characteristics of this group of PLA_2s in both crystal forms. It comprised three long α-helices (1–13, 38–55, 83–103), one double-stranded antiparallel β-sheet designated as a β-wing (68–79) and the calcium-binding loop (25–35). These structural elements as well as the C-terminal ridge are cross-linked by seven disulfide bridges (11:71, 26:118, 28:44, 43:99, 50:92, 60:85, 78:90). The structures of the active site and the hydrophobic channel are also highly conserved.

3.2. Ca^{2+} binding loop

Although the overall monomer structure is very conservative in both crystal forms, several local conformational variations were observed. For comparison, each monomer of the trimer from the tetragonal form was superimposed with the monomer of the cubic form, giving a rmsd of 0.53 Å in Cα for monomer A, 0.62 Å for monomer B and 0.61 Å for monomer C. The Ca^{2+} binding loop, the β-wing and the

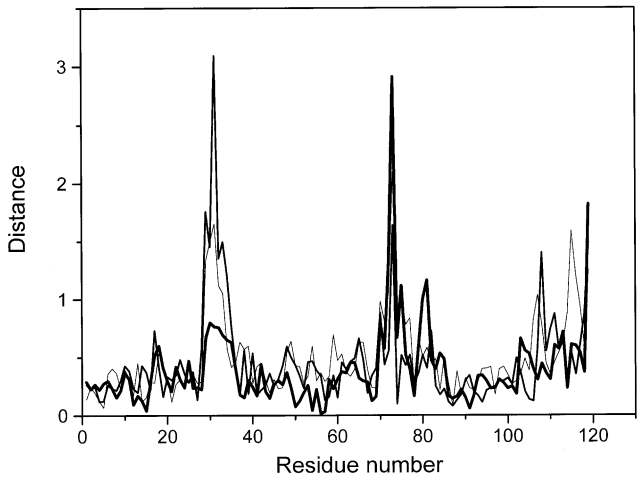

Fig. 1. Distances between Cα pairs of the monomer from the cubic form and each monomer from the tetragonal form along the polypeptide chain. The significant differences in the Ca^{2+} binding loop (25–35), the β-wing (68–79) and the C-terminal ridge (103–120) are clearly shown. Thick lines: monomer A; medium lines: monomer B; thin lines: monomer C.

C-terminal ridge all deviated significantly from the superimposed structures (Fig. 1). Similar variations were reported in the Indian cobra PLA_2 structure, in which four residues (30, 42, 73 and 119) deviated significantly. However, the Ca^{2+} binding loop in the present structure deviates to a greater extent.

The calcium ion was missing in both structures. Structural comparison of the Ca^{2+} binding loop from the cubic and tetragonal forms showed significant conformational differences (Fig. 2). In the cubic form, two oxygen atoms of the carbonyl groups from Tyr27 and Gly31 protrude inwardly toward the carboxyl groups of the Asp48. This conformation resembles that of the loop containing Ca^{2+}. In the tetragonal form, however, the oxygen atoms of the carbonyl groups from Gly29 and Gly31 protrude outwardly. The Ca^{2+} binding loop is buried inside the trimer and involved in the monomer–monomer interactions in both crystal forms. The conformational variations may be due to the breakage of strict 3-fold symmetry in tetragonal structure. This indicates that the Ca^{2+} binding loop in the absence of the cation, can exist in different conformations depending on its surroundings.

3.3. Anticoagulant site

N. kaouthia venom PLA_2 showed strong anticoagulant activity. It was suggested that the anticoagulant activity was independent of enzymatic activity and a segment of the peptide (54–66) with many positively charged residues was responsible for this pharmacological action (Boffa et al., 1976; Kini and Evans, 1987). Structure comparison showed the conformational similarity of this segment in all PLA_2 which possess strong anticoagulant activity (Singh et al., 2001). The present structure also conserved the conformation of this segment. Sequence comparison showed that the two residues Lys65 and Thr66 are highly conserved in group I PLA_2 anticoagulants.

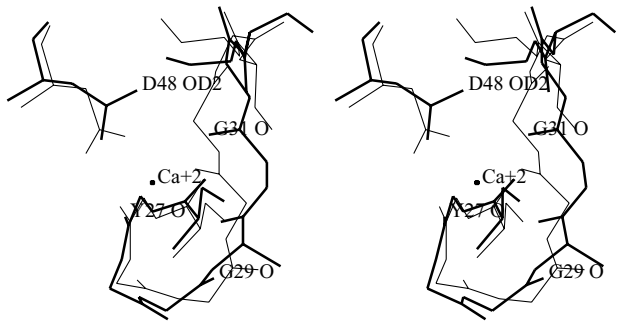

Fig. 2. Superposition of the Ca^{2+} binding loop from the cubic form (thick line) with that from the tetragonal form (molecule B, thin line). The coordinate of Ca^{2+} was taken from *N. atra* PLA_2 (PDB code: 1POA).

Fig. 3. Stereo view of the ribbons diagram of the trimer structure. The catalytic residue His47 and all the aromatic residues are shown. The three monomers form a large hydrophobic cavity in the center of the trimer.

3.4. Trimer structure

The *N. kaouthia* PLA_2 exhibits trimer structure in both crystal forms. This multimerisation state of the enzyme is similar to that of *N. naja* PLA_2; however, it differs from that of *N. atra* PLA_2, where the enzyme exists as a monomer. The monomers in *N. kaouthia* PLA_2 are related by a crystallographic 3-fold rotation axis for cubic form, but are related by a non-crystallographic 3-fold rotation axis in the tetragonal form. Superposition of the two kinds of trimers gave a rmsd of 0.92 Å for all Cα atoms, which indicates that the two structures are very similar to each other.

The trimer is stabilized by a large amount of hydrophobic and electrostatic interactions. All of the aromatic residues and most of the other hydrophobic residues located on the monomer surface are buried inside the trimer. For the cubic form, the oligomer forms a triangular prism about 38 Å high with edges of about 47 Å. The total interface area buried in by the trimer is 3454 $Å^2$ (program CCP4), corresponding to 17.8% of the monomer surface area, a value close to that of a typical trimer (Janin et al., 1988).

The most prominent feature of the trimer is a large cavity in the center (Fig. 3). The three monomers connect with each other to form the cavity wall. The three aromatic residues Phe64 related by the 3-fold rotation axis form a closed floor at the bottom of the cavity. Residues Asp113, Asn111 and Asp23 form a 8 Å long bottleneck with a 8 Å diameter at the top of the cavity. Below the bottleneck, the cavity space widens greatly and is hydrophobic being composed of residues Trp19, Ala22, Trp18, Lys63, Leu2, Tyr3 and Phe64. The cavity is about 20 Å long with a maximum diameter of about 15 Å.

4. Discussion

Protein oligomers are always of interest in X-ray crystallography due to their potential functional importance. The trimer structure in *N. kaouthia* PLA_2 is similar to that of India cobra PLA_2. The trimer observed in the crystalline state may exist in the *N. kaouthia* venom gland, which is rich in the enzyme (with a concentration of 6 mg/ml). These reinforce the physiological relevance of this oligomer.

It was suggested that the trimeric form of venom PLA_2 could represent an inactive form of the enzyme due to the inability of the substrate to reach the cavity interior (Fremont et al., 1993; Segelke et al., 1998). In the trimer, the entrance of the hydrophobic channel, which connects to the catalytic site, faces toward the trimer cavity. Careful structural inspection shows that the bottleneck of the present trimer is wide enough for the substrate to pass through. A model-building study using the phosphonate transition-state analogue of PLA_2 from the complex structure of *N. atra* PLA_2 (White et al., 1990) as a substrate showed that the substrate fits well into the trimer cavity bottleneck without close contacts (Fig. 4). So the PLA_2 molecule in the trimer state may still be active, although the catalytic activity may be weaker than that of the monomer due to the narrow bottleneck. Considering that all of the aromatic residues and most of the hydrophobic residues located on the molecule surface are buried inside the trimer, the oligomeric states of venom PLA_2s may serve as a storage method to improve the solubility at high concentrations in the venom gland.

Acknowledgements

This work was supported by the National Natural Science Foundation of China (No. 39970174). We thank Prof. Shengxi Tang for his most helpful discussion and Dr Xudong Zhao for his help during data collection and processing.

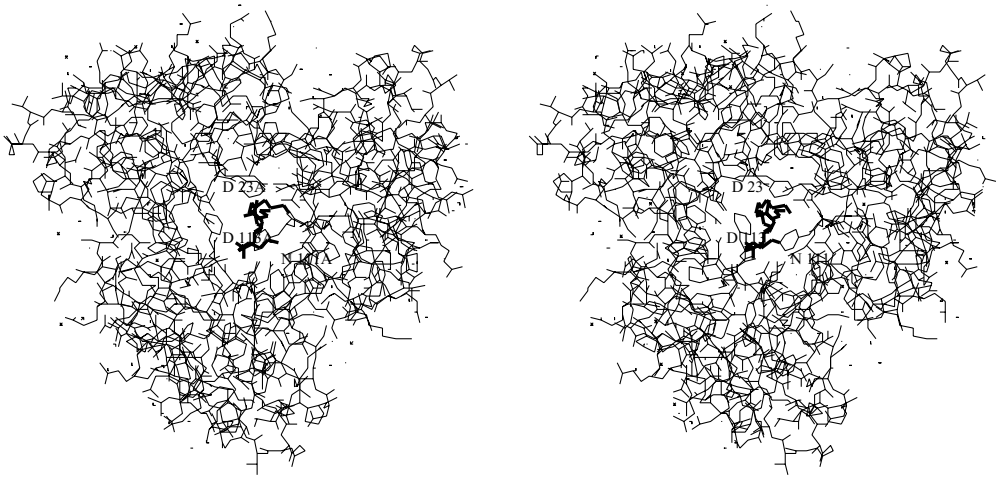

Fig. 4. Stereo view of the trimer showing the fitting of a substrate analogue (thick lines) into the cavity bottleneck.

References

Arni, R.K., Ward, R.J., Gutierrez, J.M., Tulinsky, A., 1995. Structure of a calcium-independent phospholipase-like myotoxic protein from *Bothrops asper* venom. Acta Crystallogr. D 51, 311–317.

Betzel, C., Genov, N., Rajashankar, K.R., Singh, T.P., 1999. Modulation of phospholipase A2 activity generated by molecular evolution. Cell Mol. Life Sci. 56, 384–397.

Boffa, G.A., Boff, M.C., Winchenne, J.J., 1976. A Phospholipase A2 with anticoagulant activity. I. Isolation from *Vipera berus* venom and properties. Biochim. Biophys. Acta 429, 828–836.

Brunger, A.T., 1992. Free *R* value: anoval statistical quantity for assessing the accuracy of crystal structures. Nature 355, 472–475.

Brunger, A.T., Adams, P.D., Clore, G.M., DeLano, W.L., Gros, P., Grosse-Kunstleve, R.W., Jiang, J.S., et al., 1998. Crystallography and NMR system: a new software suite for macromolecular structure determination. Acta Crystallogr. D 54, 905–921.

Brunie, S., Bolin, J., Gewirth, D., Sigler, P.B., 1985. The refined crystal structure of dimeric phospholipase A2 at 2.5 Å. Access to a shielded catalytic center. J. Biol. Chem. 260, 9742–9749.

Dufton, M.J., Hider, R.C., 1983. Classification of phospholipases A2 according to sequence. Evolutionary and pharmacological implications. Eur. J. Biochem. 137, 545–551.

Fremont, D.H., Anderson, D.H., Wilson, I.A., Dennis, E.A., Xuong, N.H., 1993. Crystal structure of phospholipase A2 from Indian cobra reveals a trimeric association. Proc. Natl. Acad. Sci. USA 90, 342–346.

Gowda, V.T., Schmidt, J., Middlebrook, J.L., 1994. Primary sequence determination of the most basic myonecrotic phospholipase A2 from the venom of *Vipera russelli*. Toxicon 32, 665–673.

Heinrikson, R.L., Krueger, E.T., Keim, P.S., 1977. Amino acid sequence of phospholipase A2-alpha from the venom of *Crotalus adamanteus*. A new classification of phospholipases A2 based upon structural determinants. J. Biol. Chem. 252, 4913–4921.

Janin, J., Miller, S., Chothia, C., 1988. Surface, subunit interfaces and interior of oligomeric proteins. J. Mol. Biol. 204, 155–164.

Joubert, F.J., Taljaard, N., 1980. Purification, some properties and amino-acid sequences of two phospholipases A (CM-II and CM-III) from *Naja kaouthia* venom. Eur. J. Biochem. 112, 493–499.

Kini, R.M., Evans, H.J., 1987. Structure–function relation of phospholipases. The anticoagulant region of phospholipase A2. J. Biol. Chem. 262, 14402–14407.

Laskowski, R., Macarthur, M., Moss, D., Thornton, J., 1993. Procheck: a program to check stereochemical quality of protein structures. J. Appl. Crystallogr. 26, 283–290.

Matthews, B.W., 1968. Solvent content of protein crystals. J. Mol. Biol. 33, 491–497.

Otwinowski, Z., Minor, W., 1997. Processing of X-ray diffraction data collected in oscillation mode. Meth. Enzymol. 276, 307–326.

Pluckthun, A., Dennis, E.A., 1985. Activation, aggregation, and product inhibition of cobra venom phospholipase A2 and comparison with other phospholipases. J. Biol. Chem. 260, 11099–11106.

Segelke, B.W., Nguyen, D., Chee, R., Xuong, N.H., Dennis, E.A., 1998. Structures of two novel crystal forms of *Naja naja* naja phospholipase A2 lacking Ca^{2+} reveal trimeric packing. J. Mol. Biol. 279, 223–232.

Singh, G., Gourinath, S., Sharma, S., Paramasivam, M., Srinivasan, A., Singh, T.P., 2001. Sequence and crystal structure determination of a basic phospholipase A2 from common krait (*Bungarus caeruleus*) at 2.4 Å resolution: identification and characterization of its pharmacological sites. J. Mol. Biol. 307, 1049–1059.

Tang, L., Zhou, Y.C., Lin, Z.J., 1998. Crystal structure of agkistrodotoxin, a phospholipase A2-type presynaptic neurotoxin from *Agkistrodon halys* pallas. J. Mol. Biol. 282, 1–11.

Wang, Z.Q., 1999. MS Thesis, Guangxi Medical University, China.

Wang, X.Q., Yang, J., Gui, L.L., Lin, Z.J., Chen, Y.C., Zhou, Y.C., 1996. Crystal structure of an acidic phospholipase A2 from the venom of *Agkistrodon halys* pallas at 2.0 Å resolution. J. Mol. Biol. 255, 669–676.

Wang, Z.Q., Zhuang, M.X., Song, S.Y., Lin, Z.J., Shu, Y.Y., 2001. Preliminary crystallographic analysis of phospholipase A2 from *Naja naja* kaouthia lesson Venom. Acta Biochim. Biophys. Sinica 33, 582–584.

White, S.P., Scott, D.L., Otwinowski, Z., Gelb, M.H., Sigler, P.B., 1990. Crystal structure of cobra-venom phospholipase A2 in a complex with a transition-state analogue. Science 250, 1560–1563.